Magnetic moments of Λ hypernuclei within the time-odd triaxial relativistic mean-field approach

H. Y. Sang,[1] X. S. Wang,[1] H. F. Lü,[1,*] J. M. Yao,[2] and H. Sagawa[3]
[1]*College of Science, China Agriculture University, Beijing 100083, China*
[2]*School of Physical Science and Technology, Southwest University, Chongqing 400715, China*
[3]*Center for Mathematical Sciences, University of Aizu, Ikki-machi, Aizu-Wakamatsu, Fukushima 965-8580, Japan*
(Received 21 September 2013; revised manuscript received 8 November 2013; published 3 December 2013)

Λ-hypernuclear magnetic moments have been studied self-consistently in time-odd triaxial relativistic mean-field approach with newly proposed Λ-meson interactions. The $\omega\Lambda\Lambda$ tensor coupling highly reduces the polarized Dirac magnetic moment. The deviation of the magnetic moment from the Schmidt value $\Delta\mu$ is related to effective nucleon-meson interaction. A large deviation $\Delta\mu$ with $l_\Lambda \neq 0$ is found to exist only in medium-mass hypernuclei.

DOI: 10.1103/PhysRevC.88.064304 PACS number(s): 21.10.Ky, 21.30.Fe, 21.60.Jz, 21.80.+a

I. INTRODUCTION

The magnetic moment provides a highly sensitive probe of single-particle structure and serves as a stringent test of nuclear models. The hypernuclear magnetic moment can further provide direct information about hyperon-nucleon interaction and the role of hadrons in nuclear medium [1,2]. Measurement of the hypernuclear magnetic moment may shed light on the Λ-meson interaction in hypernuclei and provides a way to penetrate various theoretical models. With technique development, measurements of hypernuclear magnetic moments are in process [3–5].

The Λ spin-flip $M1$ transition probability $B(M1)$ in ${}^{11}_{\Lambda}$B $(3/2^+ \to 1/2^+)$, in ${}^{7}_{\Lambda}$Li $(7/2^+ \to 5/2^+, 3/2^+ \to 1/2^+)$, and in ${}^{9}_{\Lambda}$Be$(3/2^+ \to 1/2^+)$ has been studied with Hyperball in the (π^+, K^+) reaction at KEK [2,6]. The $M1$ $(1^-_2 \to 1^-_1, 0^-)$ transition of ${}^{16}_{\Lambda}$O using the (K^-, π^-) reaction has also been studied at BNL (E930) [7]. The systematic study of the magnetic moment for a wide mass range of Λ hypernuclei has been carried out at a hypernuclear physics program with relativistic heavy ion beams, HypHI Phase 3 [8].

Therefore, a reliable theoretical approach for the accurate description of hypernuclear magnetic moments is urgently required. An approach based on the relativistic mean-field (RMF) provides a very interesting theoretical framework for studies of nuclear structure phenomena at and far from the valley of β stability [9–12]. So far, RMF theory has been applied to investigate hypernuclear magnetic moments, such as the self-consistent spherical RMF approach plus linear core response approximation [13,14] and perturbation treatment [15,16], the spherical RMF approach with $\omega\Lambda\Lambda$ tensor coupling based on a phenomenological Woods-Saxon potential [17], or the self-consistent time-odd axial RMF approach [18]. However, a self-consistent study of hypernuclear magnetic moments using a RMF approach with both a nonzero spacelike (time-odd) component of the vector field and $\omega\Lambda\Lambda$ tensor coupling is still missing.

To investigate the self-consistent effects of a spacelike component, $\omega\Lambda\Lambda$ tensor coupling, and core polarization, a triaxial RMF approach with strangeness, odd-time components, and meson-hyperon vertex is presented in contrast with the previous perturbation treatment. Newly developed meson-baryon interaction with proton-neutron mass difference PK1-Y1, PK1-Y2, PK1-Y3, and PK1-Y0 are used, which are determined via both the hyperon binding energy and the hyperon spin-orbit splitting [19]. The interactions are optimized based on meson-nucleon interaction PK1 [20] by considering the $\omega\Lambda\Lambda$ tensor, the proton-neutron mass difference, and microscopic correction for the spurious center-of-mass motion. The distribution of core-polarized proton current, the influence on magnetic moments from $\omega\Lambda\Lambda$ coupling, and the sensitivity of magnetic moments on effective interaction are studied. Systems of one Λ hyperon plus even-even core nuclei, odd-A core nuclei, or odd-odd core nuclei are included.

The paper is arranged as follows: In Sec. II, the theoretical framework of the time-odd triaxial RMF approach with strangeness and the $\omega\Lambda\Lambda$ tensor coupling term is introduced briefly. The effects of $\omega\Lambda\Lambda$ tensor coupling, core polarization, and effective meson-baryon interaction on hypernuclear current and magnetic moment are studied in Sec. III. Finally, a summary is given in Sec. IV.

II. THEORETICAL FRAMEWORK

The starting point of RMF theory is the standard effective Lagrangian density constructed with degrees of freedom associated with the baryon field (ψ_B), two isoscalar meson fields (σ and ω), the isovector meson field (ρ), and the photon field (A) [9–12]. For Λ hypernuclei, it is generalized by including a tensor coupling term $\frac{f_{\omega BB}}{4m_B}\bar{\psi}_B\sigma^{\mu\nu}\Omega_{\mu\nu}\psi_B$ as [21]

$$\begin{aligned}\mathcal{L} = \bar{\psi}_B\Big[& i\gamma^\mu\partial_\mu - m_B - g_{\sigma B}\sigma - g_{\omega B}\gamma^\mu\omega_\mu \\ & + \frac{f_{\omega BB}}{4m_B}\sigma^{\mu\nu}\Omega_{\mu\nu} - g_{\rho B}\gamma^\mu\vec{\tau}\cdot\vec{\rho}_\mu - Q_B\gamma^\mu A_\mu\Big]\psi_B \\ & + \frac{1}{2}\partial_\mu\sigma\partial^\mu\sigma - \frac{1}{2}m_\sigma^2\sigma^2 - \frac{1}{3}g_2\sigma^3 - \frac{1}{4}g_3\sigma^4 \\ & - \frac{1}{4}\Omega_{\mu\nu}\Omega^{\mu\nu} + \frac{1}{2}m_\omega^2\omega_\mu\omega^\mu + \frac{1}{4}c_3(\omega_\mu\omega^\mu)^2 \\ & - \frac{1}{4}\vec{R}_{\mu\nu}\vec{R}^{\mu\nu} + \frac{1}{2}m_\rho^2\vec{\rho}_\mu\cdot\vec{\rho}^\mu - \frac{1}{4}F_{\mu\nu}F^{\mu\nu}, \end{aligned} \quad (1)$$

where $\sigma^{\mu\nu} = \frac{1}{2i}[\gamma^\mu, \gamma^\nu]$, and m_B ($B = n, p, \Lambda$) and m_ϕ($\phi = \sigma, \omega, \rho$) are masses of baryons and mesons, respectively. The

*hongfeng@cau.edu.cn

 ©2013 American Physical Society

field tensor for the ω meson is given as $\Omega_{\mu\nu} = \partial_\mu \omega_\nu - \partial_\nu \omega_\mu$ and by similar expressions for ρ mesons and photons. Q_B is the charge of baryons.

The Dirac equation of baryons and the Klein-Gordon equation for mesons can be derived from the Lagrangian density in Eq. (1) with a variational principle as

$$i\gamma_\mu \partial^\mu \psi_B = \left[\gamma_\mu V_B^\mu + (m_B + S_B) - \frac{f_{\omega BB}}{4m_B}\sigma_{\mu\nu}\Omega^{\mu\nu}\right]\psi_B, \tag{2a}$$

$$\left(\partial^\mu \partial_\mu + m_\omega^2\right)\omega_\mu = \bar{\psi}_B g_{\omega B}\gamma_\mu \psi_B - c_3 \omega_\nu \omega^\nu \omega_\mu + \frac{f_{\omega BB}}{2m_B}\partial^\mu(\bar{\psi}_B \sigma_{\mu\nu}\psi), \tag{2b}$$

where the scalar potential S_B and the vector potential V_B^μ are given by $S_B = g_{\sigma B}\sigma$ and $V_B^\mu = g_{\omega B}\omega^\mu + g_{\rho B}\tau_3 \rho_3^\mu + Q_B A^\mu$. As the ωBB tensor couplings are negligible for nucleons [21], here only $\omega\Lambda\Lambda$ tensor coupling is considered. Equations of motion for meson fields σ and ρ and photon field A can be derived in similar way.

In the mean-field approximation, meson fields and photon fields are treated as classical fields. Therefore, equations of motion for meson fields become the classical time-independent inhomogeneous Klein-Gordon equations.

Due to odd valence baryons, spacelike components of the vector field break the time reversal invariance in nuclear states and result in a nonvanishing proton current in the RMF approach, further deviating the magnetic moment from the corresponding Schmidt value. The effective electromagnetic current operator is given by [22]

$$\hat{J}_B^{\mu,\mathrm{em}}(x) = Q_B \bar{\psi}(x)\gamma^\mu \psi(x) + \frac{\kappa}{2m_B}\partial_\nu[\bar{\psi}(x)\sigma^{\mu\nu}\psi(x)], \tag{3}$$

where field operators are in the Heisenberg representation with κ, free anomalous gyromagnetic ratio of the baryon (in units of the nuclear magneton μ_N): $\kappa^p = 1.793$, $\kappa^n = -1.913$, and $\kappa^\Lambda = -0.613$. The current operator in Eq. (3) is explicitly conserved by antisymmetry of $\sigma^{\mu\nu}$ and virtue of the relativistic Hartree equations for a nucleus. The spacelike components of $\hat{J}_B^{\mu,\mathrm{em}}(x)$ in the Schrödinger picture reduce to

$$\hat{\mathbf{J}}_B^{\mathrm{em}}(\mathbf{r}) = Q_B \psi^\dagger(\mathbf{r})\boldsymbol{\alpha}\psi(\mathbf{r}) + \frac{\kappa}{2m_B}\nabla \times [\psi^\dagger(\mathbf{r})\beta\boldsymbol{\Sigma}\psi(\mathbf{r})]. \tag{4}$$

The matrix element in the Hartree approximation becomes [23]

$$\left\langle \hat{\mathbf{J}}_B^{\mathrm{em}}(\mathbf{r})\right\rangle = \sum_{k>0} Q_B \psi_k^\dagger(\mathbf{r})\boldsymbol{\alpha}\psi_k(\mathbf{r}) + \frac{\kappa}{2m_B}\nabla \times \sum_{k>0}\psi_k^\dagger(\mathbf{r})\beta\boldsymbol{\Sigma}\psi_k(\mathbf{r}), \tag{5}$$

where $\psi_k(\mathbf{r})$ is the single baryon wave function. The first term in Eq. (5) without Q_B is the Dirac current, $\mathbf{J}_D(\mathbf{r}) \equiv \sum_{k>0}\psi_k^\dagger(\mathbf{r})\boldsymbol{\alpha}\psi_k(\mathbf{r})$, and the second term is the anomalous one, $\mathbf{J}_a$. With no charge, the Dirac currents of neutrons and Λ hyperons have no contribution to the hypernuclear electromagnetic moment.

The magnetic moment can be calculated from the matrix element of the current in Eq. (5) as $\mu = \frac{1}{2}\int d^3r \mathbf{r} \times \langle \hat{\mathbf{J}}_B^{\mathrm{em}}(\mathbf{r})\rangle$, which can be divided into two terms:
the Dirac magnetic moment,

$$\mu_D = \sum_{k>0}\frac{m_B c^2}{\hbar c}\int d^3r\, Q_B \psi_k^\dagger(\mathbf{r})\mathbf{r} \times \boldsymbol{\alpha}\psi_k(\mathbf{r}), \tag{6}$$

and the anomalous magnetic moment,

$$\mu_a = \sum_{k>0}\kappa \int d^3r \psi_k^\dagger(\mathbf{r})\beta\Sigma\psi_k(\mathbf{r}). \tag{7}$$

As $\beta\Sigma$ does not mix the upper and lower components of the Dirac spinor, the elementary anomalous current contribution is not appreciable [15]. In the following, we mainly discuss the Dirac magnetic moment.

III. RESULTS AND DISCUSSION

The harmonic oscillator basis expansion method has been used to solve the Dirac equation, Eq. (2a), for baryons and the Klein-Gordon equations for meson fields (σ, ω, ρ), which are expanded on a three-dimensional harmonic oscillator basis in Cartesian coordinates discretized with Gaussian-Hermite mesh points. The electromagnetic field is solved using the standard Green's function method due to its long-range characters. For a system with an odd baryon number, time-odd components of the vector field appear and the Dirac equations have to be solved separately in two subspaces with different simplexes. Major shell numbers are chosen as $n_f = 12$ and $n_b = 10$ for baryons and mesons, respectively. Gaussian mesh points are chosen as $n_{\mathrm{gh}} = 12$ and the first mesh point in the calculation is $x(y, z) = 0.36$ fm. More numerical details can be found in Ref. [24]. To focus on the effects of the time-odd component and the tensor coupling term, particle occupation is taken from the bottom of the well and the pairing effect is shielded.

The effective meson-baryon interactions PK1-Y0, PK1-Y1, PK1-Y2, etc. [19], based on the meson-nucleon interaction PK1 [20], are used. The coupling strength ratios of Λ-mesons, $R_\sigma = g_{\sigma\Lambda}/g_{\sigma N}$ and $R_\omega = g_{\omega\Lambda}/g_{\omega N}$ with $f_{\omega\Lambda\Lambda} = 0$ or $f_{\omega\Lambda\Lambda} = g_{\omega\Lambda}$, are searched by fitting Λ single-particle energies and p_Λ spin-orbit splittings.

In Table I, the optimal parameter sets; time-reversal single-particle energies of the $1s_\Lambda$ state and their splitting; Dirac, anomalous and total magnetic moments for $^{17}_{\Lambda}$O in the time-odd triaxial RMF approach; and the general agreement $S(\Delta)$ with the Λ single-particle energies are respectively given. In Table I, the splitting between time-reversal states of $1s_\Lambda$ is reduced from roughly 0.1 to 0.02 MeV by switching on the $\omega\Lambda\Lambda$ tensor coupling. Tensor coupling affects the spatial distribution of particles. In Eq. (2), the response to the Λ-hyperon results from the spacelike component of the ω meson and from $\omega\Lambda\Lambda$ tensor coupling. Taking $^{17}_{\Lambda}$O as an example, the Λ-hyperon single-particle spectrum ($l_\Lambda = 1$) is shown in Fig. 1. Obviously, time-odd contribution splits states in two subspaces (spin doublet) by the antipair effect while $\omega\Lambda\Lambda$ tensor coupling plays a great role in the small spin-orbit splitting of the Λ hyperon. The

TABLE I. Λ single-particle energy and Dirac, anomalous, and total magnetic moments in ${}^{17}_{\Lambda}$O. Results are obtained with the time-odd triaxial RMF approach with several parameters sets [19]. Coupling-strength ratios are defined as $R_\sigma \equiv g_{\sigma\Lambda}/g_{\sigma N}$ and $R_\omega \equiv g_{\omega\Lambda}/g_{\omega N}$. Λ single-particle energies for time-reversed partners (T^+ and T^-) and their splitting are shown by ε_Λ and $\Delta\varepsilon_\Lambda$, respectively. The Schmidt value of ${}^{17}_{\Lambda}$O is $-0.613\ \mu_N$.

Sets	$f_{\omega\Lambda\Lambda}$	R_σ	R_ω	ε_Λ (MeV)		$\Delta\varepsilon_\Lambda$	Magnetic moment (μ_N)			$S(\Delta)$[a]
				T^+	T^-		μ_D	μ_a^Λ	$\mu_{\rm tot.}$	
PK1-Y1		0.580	0.620	−12.700	−12.683	0.017	−0.009	−0.610	−0.619	0.054(0.851)
PK1-Y2	$g_{\omega\Lambda}$	0.705	0.772	−12.585	−12.564	0.021	−0.012	−0.610	−0.622	0.051(0.815)
PK1-Y3		0.400	0.400	−13.229	−13.218	0.011	−0.004	−0.610	−0.614	0.085(1.225)
PK1-Y0	0	0.840	0.940	−12.838	−12.730	−0.108	−0.054	−0.610	−0.664	0.048(0.749)

[a]Uncertainty deviations: $S \equiv \sqrt{\frac{1}{N}\sum_{i=1}^{N}\frac{(\varepsilon_i^{\rm exp.}-\varepsilon_i^{\rm cal.})^2}{(\varepsilon_i^{\rm exp.})^2}}$, $\Delta \equiv \sqrt{\frac{1}{N}\sum_{i=1}^{N}(\varepsilon_i^{\rm exp.}-\varepsilon_i^{\rm cal.})^2}$.

energy shift caused by the time-odd component and $\omega\Lambda\Lambda$ tensor coupling will be important in the nuclear transition.

With no $\omega\Lambda\Lambda$ tensor coupling ($f_{\omega\Lambda\Lambda} = 0$), the polarized Dirac magnetic moment μ_D is about 7% of the total magnetic moment $\mu_{\rm tot.}$, which leads to a large deviation from the Schmidt value $-0.613\ \mu_N$ (see results obtained with PK1-Y0 in Table I). Considering $\omega\Lambda\Lambda$ tensor coupling, the polarized Dirac magnetic moment is reduced and results in a shrinkage of the total magnetic moment. Obviously, the presence of $\omega\Lambda\Lambda$ tensor coupling will modify the current vertex and suppress the effect of core polarization on the magnetic moments [14,25]. With a $\omega\Lambda\Lambda$ tensor coupling, the magnetic moment of the Λ hypernucleus with $l_\Lambda = 0$ is restored to the Schmidt value [16,17] (see results obtained with PK1-Y1, PK1-Y2, and PK1-Y3 in Table I). This confirms the prediction based on a phenomenological Woods-Saxon potential and a $\omega\Lambda\Lambda$ tensor coupling [17].

To investigate the response of the core to the valence neutron and the Λ hyperon, the polarized Dirac currents of proton $\mathbf{J}_D^p$ in ${}^{17}_{\Lambda}$O and in ^{17}O around the yz plane at $x = 0.36$ fm are given in Fig. 2. They are obtained with meson-baryon interaction PK1-Y1 for ${}^{17}_{\Lambda}$O (upper panel) and ^{17}O (lower panel), respectively.

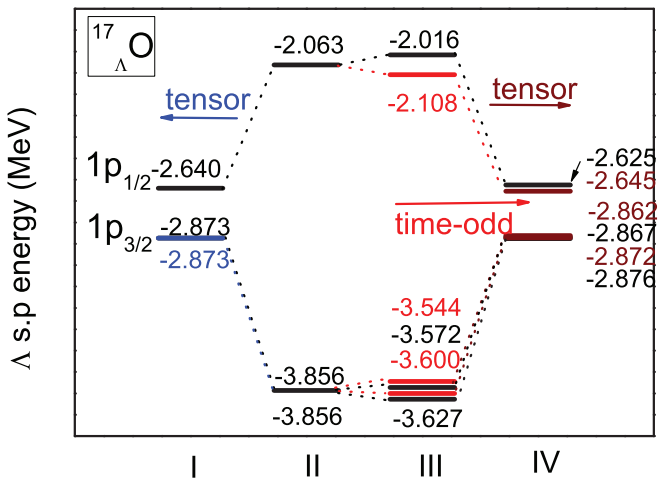

FIG. 1. (Color online) Effects on the single-particle spectrum of Λ in ${}^{17}_{\Lambda}$O from the spacelike component of the ω meson and from $\omega\Lambda\Lambda$ tensor coupling. Results are obtained using the time-odd triaxial RMF approach with the parameter set PK1-Y1 [19].

The current $\mathbf{J}_D^p$ (y) at $x = z = 0.36$ fm is presented by the corresponding spline curves with arbitrary scale. The peak of $\mathbf{J}_D^p(y)$ around $y = 0.36$ fm in ${}^{17}_{\Lambda}$O is about 1.21×10^{-5} fm^{-3} while that in ^{17}O is about 0.82×10^{-2} fm^{-3}. As the Λ hyperon stays at the $1s$ state, the Λ current distributes mainly in the interior of the ^{16}O core and the valence Λ hyperon shows a diffusion effect of $\mathbf{J}_D^p$; see the inner clockwise current radius ∼1 fm in ${}^{17}_{\Lambda}$O and ∼0.3 fm in ^{17}O. Thus, for a Λ hyperon at

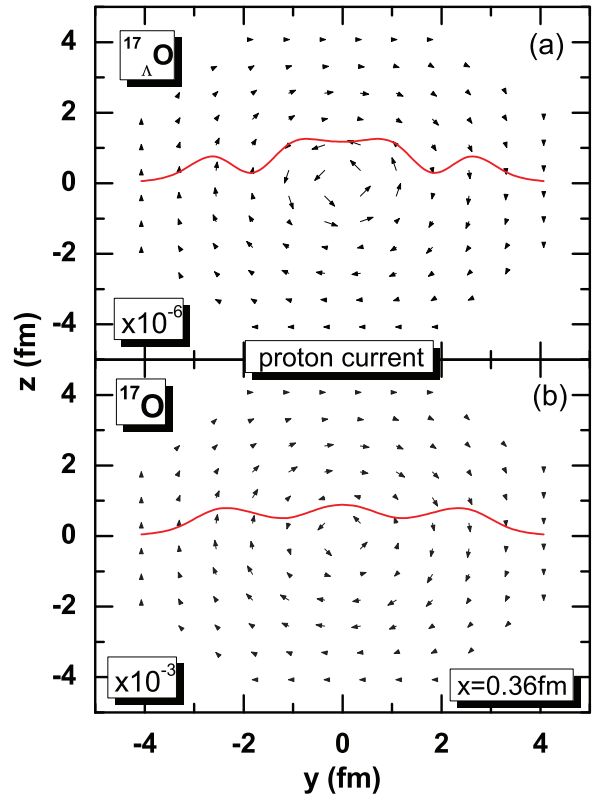

FIG. 2. (Color online) Core polarized proton currents in the yz plane at $x = 0.36$ fm obtained by the time-odd triaxial RMF approach with PK1-Y1 for ${}^{17}_{\Lambda}$O (upper panel) and ^{17}O (lower panel). The direction and the length of the arrows represent the orientation and the magnitude of the currents, respectively. Corresponding spline curves are the currents at $x = z = 0.36$ fm with arbitrary scale. Data for ${}^{17}_{\Lambda}$O and ^{17}O in the figure are zoomed in 10^6 times and 10^3 times, respectively.

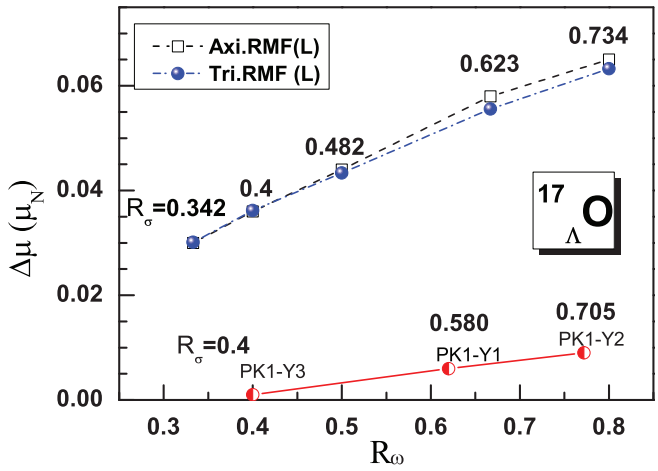

FIG. 3. (Color online) Relationship between deviation $\Delta\mu$ and coupling constant ratios R_σ and R_ω. Results using the axial (taken from Ref. [18]) and triaxial RMF approaches with the L set are denoted with open squares and solid circles, respectively. Predictions using the triaxial RMF approach with $\omega\Lambda\Lambda$ tensor coupling are also presented by half-filled circles.

the 1s state, the core contribution to the magnetic moment is small and the resulting hypernuclear magnetic moment comes very close to the Schmidt value.

Under a perturbation treatment from nuclear matter, the core-polarized magnetic moment in the Λ hypernucleus with $\omega\Lambda\Lambda$ tensor coupling is proportional to the meson-baryon coupling strength $g_{\omega N}g^2_{\omega\Lambda}$ approximately [15,17]. Besides a modified expression of the polarized Dirac magnetic moment, we further improved the result by a self-consistent calculation of the meson potentials and show a semilinear relation between the polarized magnetic moment and the meson-Λ coupling strength $g_{\omega\Lambda}$ [16]. However, self-consistent treatment of the spacelike component and $\omega\Lambda\Lambda$ tensor coupling is missing in previous studies. Considering both the spacelike component and the $\omega\Lambda\Lambda$ tensor coupling, sensitivity of the magnetic moment to coupling strengths may show a different look.

In Fig. 3, the deviation of a magnetic moment from the corresponding Schmidt value $\Delta\mu$ as a function of R_σ and/or R_ω is shown. The time-odd axial RMF values [Axi.RMF(L)] denoted with open squares are directly taken from Ref. [18] and the time-odd triaxial RMF results [Tri.RMF(L)] with the L set are denoted with solid circles. Obviously, Axi.RMF(L) and Tri.RMF(L) match each other quite well for the spherical nucleus $^{17}_{\Lambda}$O. Results in the odd-time triaxial RMF approach with parameter sets PK1-Y1, PK1-Y2, and PK1-Y3 are also listed. The suppression effect of core polarization on the magnetic moments from the $\omega\Lambda\Lambda$ tensor is clearly shown. The anomalous current of the valence baryon is not sensitive to effective mass $m^* = \langle m - g_{\sigma B}\sigma\rangle$ with no mixing between the upper and lower components of the Dirac spinor [25]. The anomalous magnetic moment is near the Schmidt value in the spherical case and is insensitive to the Λ-nucleon interaction due to the small effect from the lower component in the Dirac spinor [26]. The Dirac magnetic moment plays a major role in the meson-baryon interaction dependence.

TABLE II. Magnetic moments of oxygen hypernuclei in units of nucleon magneton (μ_N), obtained by using the time-odd triaxial RMF approach with PK1 and PK1-Y1. The hypernuclear magnetic moment $\mu_{\text{tot.}}$ is the sum of the Dirac magnetic moment μ_D and the anomalous magnetic moments μ_a^{n+p} and μ_a^{Λ}. The Schmidt magnetic moment is denoted by $\mu_{\text{Sch.}}$.

System	μ_D	μ_a^{n+p}	μ_a^{Λ}	$\mu_{\text{tot.}}$	$\mu_{\text{Sch.}}$
^{15}O + free Λ	−0.113 [24]	0.677 [24]	−0.613	−0.049	0.025
$^{16}_{\Lambda}$O(PK1-Y1)	−0.130	0.681	−0.610	−0.060	0.025
$^{16}_{\Lambda}$O(PK1-Y0)	−0.179	0.690	−0.610	−0.099	0.025
^{16}O + free Λ	0.0	0.0	−0.613	−0.613	−0.613
$^{17}_{\Lambda}$O(PK1-Y1)	−0.009	0.0	−0.610	−0.619	−0.613
$^{17}_{\Lambda}$O(PK1-Y0)	−0.054	0.0	−0.610	−0.664	−0.613
^{17}O + free Λ	−0.134 [24]	−1.863 [24]	−0.613	−2.610	−2.526
$^{18}_{\Lambda}$O(PK1-Y1)	−0.144	−1.864	−0.610	−2.618	−2.526
$^{18}_{\Lambda}$O(PK1-Y0)	−0.192	−1.863	−0.610	−2.665	−2.526

The polarized Dirac magnetic moment is found to increase with the ω-Λ coupling strength $g_{\omega\Lambda}$ with or without the $\omega\Lambda\Lambda$ tensor coupling. The present results confirm previous investigation that the polarized Dirac magnetic moment is nearly proportional to the ω-Λ coupling strength $g_{\omega\Lambda}$ [16]. It is emphasized that the σ-Λ coupling strength $g_{\sigma\Lambda}$ is also associated with the polarized Dirac magnetic moment, which is consistent with the hypernuclear magnetic moment being sensitive to variations of the effective mass m^* [13]. The large coupling strength ratio R_σ increases the sensitivity of R_ω to the magnetic moment deviation $\Delta\mu$, due to the central mean-field potential $\langle g_{\sigma\Lambda}\sigma + g_{\omega\Lambda}\omega\rangle$.

To further examine the effects of the core polarization from valence Λ and $\omega\Lambda\Lambda$ tensor coupling, magnetic moments of $^{16}_{\Lambda}$O, $^{17}_{\Lambda}$O, and $^{18}_{\Lambda}$O calculated with PK1-Y0 and PK1-Y1 are given in Table II. For comparison, the magnetic moments of the corresponding core nuclei (^{15}O, ^{16}O, and ^{17}O) and the magnetic moment of the free Λ are presented. The valence hyperon in nuclear medium will produce a nonvanishing proton current and deviate the magnetic moment from the Schmidt value. From Table II, it is shown that the valence Λ hyperon enlarges the magnitude of the Dirac magnetic moment μ_D while $\omega\Lambda\Lambda$ tensor coupling reduces it. The Dirac magnetic moment μ_D of $^{16}_{\Lambda}$O calculated with PK1-Y0 diverge from that of ^{15}O + free Λ by ∼60%. Even including the $\omega\Lambda\Lambda$ tensor coupling (PK1-Y1), there is still a gap of ∼20% left. Results are similar for $^{18}_{\Lambda}$O. Thus, the core polarization effect of the valence Λ hyperon is hard to ignore. Naive treatment of the magnetic moment in the hypernucleus as a nuclear core plus a valence hyperon is questionable.

The Schmidt value $\mu_{\text{Sch.}}$ and the magnetic moment $\mu_{\text{tot.}}$ of $^{16}_{\Lambda}$O in Table II are very different, with opposite signs. The self-consistent result $-0.060\ \mu_N$ calculated with PK1-Y1 is also a reversed sign from $0.071\ \mu_N$ obtained by a summation of the measured magnetic moment for ^{15}O and a free hyperon [15] and from $0.014\ \mu_N$ acquired under improved perturbation treatment with PK1-Y1 [16]. To avoid model dependence, magnetic moments with other RMF parameter sets have been predicted. Using $g_{\sigma\Lambda} = 0.621$, $g_{\omega\Lambda} = 2/3$, and $f_{\omega\Lambda\Lambda} = 1$ for

TABLE III. Magnetic moments of hypernuclei (in units of μ_N) calculated with the parameter set PK1-Y1 using a time-odd triaxial RMF approach and a perturbation treatment (marked by ♭) [16]. The contribution from the nuclear core is presented by $\mu_{\rm core} = \mu_a^{n+p} + \mu_D$. The Schmidt values are also listed for comparison. The shape of the nuclei is shown by quadrupole deformation (β, γ).

Nuclei	μ_Λ	$\mu_\Lambda^\flat$	μ_D	$\mu_{\rm core}$	$\mu_{\rm core}^\flat$	$\mu_{\rm tot.}$	$\mu^\flat$	$\mu_{\rm Sch.}$	(β, γ)
${}^{17}_{\Lambda}$O	−0.6098	−0.6113	−0.0086	−0.0086	0	−0.6184	−0.6113	−0.6130	(0.000, 22.850)
${}^{41}_{\Lambda}$Ca	−0.6102	−0.6114	−0.0136	−0.0136	0	−0.6238	−0.6114	−0.6130	(0.000, 27.741)
${}^{209}_{\Lambda}$Pb	−0.6116	−0.6121	−0.0156	−0.0156	0	−0.6272	−0.6121	−0.6130	(0.000, 29.849)
${}^{16}_{\Lambda}$O	−0.6096	−0.6112	−0.1305	0.5504	0.6249	−0.0592	0.0137	0.0247	(−0.002, 0.396)
${}^{28}_{\Lambda}$Al	−0.6093	−0.6108	2.7730	4.4122	5.2627	3.8029	4.6519	4.1800	(0.065, 44.602)
${}^{28}_{\Lambda}$Si	−0.6094	−0.6108	−0.0518	−0.8463	−2.0439	−1.4557	−2.6547	−2.5260	(0.185, 46.600)
${}^{32}_{\Lambda}$S	−0.6097	−0.6109	−0.0464	0.8130	−1.8814	0.2022	−2.4923	−2.5260	(−0.107, 1.148)
${}^{40}_{\Lambda}$Ca	−0.6101	−0.6113	−0.2216	0.8337	1.0395	0.2236	0.4282	0.5348	(−0.034, 55.120)
${}^{51}_{\Lambda}$V	−0.6103	−0.6113	0.0081	0.0179	4.3059	−0.5924	3.6947	3.2670	(−0.089, 0.025)
${}^{89}_{\Lambda}$Y	−0.6108	−0.6116	−0.1046	−3.1027	−2.1990	−3.7135	−2.8103	−2.7903	(−0.016, 0.174)
${}^{139}_{\Lambda}$La	−0.6113	−0.6119	3.9235	0.8379	1.1805	0.2266	0.5686	−0.8094	(−0.015, 0.819)
${}^{208}_{\Lambda}$Pb	−0.6116	−0.6121	−0.1325	0.4976	0.6306	−0.1114	0.0185	0.0247	(0.000, 16.672)

meson-hyperon interaction, NLSH [27] and NL3 [28] results in units of μ_N are listed as

Sets	μ_D	μ_a^{n+p}	μ_a^Λ	$\mu_{\rm tot.}$	$\mu_{\rm Sch.}$
NLSH	−0.137	0.680	−0.610	−0.067	0.025
NL3	−0.131	0.674	−0.610	−0.067	0.025

The opposite sign between $\mu_{\rm tot.}$ and $\mu_{\rm Sch.}$ in ${}^{16}_{\Lambda}$O still exists. This may be a signal for future experiments to study because hypernuclear magnetic moments can show information about the medium Λ-meson interaction.

To find the difference between predictions from time-odd triaxial RMF and from spherical RMF with a perturbation treatment [16], systematic evaluations of hypernuclear magnetic moments are shown in Table III. The mark ♭ denotes the backflow electromagnetic current caused by core polarization from the external particle [13]. The contribution from the nuclear core is presented by $\mu_{\rm core} = \mu_a^{n+p} + \mu_D$. The Schmidt values are also listed for reference. The deviation $\Delta\mu$ is small and increases as mass number A gets larger for a double-closed shell core hypernuclei (the first three rows). Coupling strengths $g_{\sigma\Lambda}$ and $g_{\omega\Lambda}$ in the central mean-field potential $\langle g_{\sigma\Lambda}\sigma + g_{\omega\Lambda}\omega\rangle$ vary according to the binding energy in different Λ hypernuclei. The larger the mass number A is, the deeper the central potential is and the larger the meson-hyperon interaction is. This is consistent with the conclusion from Fig. 3. The anomalous μ_a^Λ is around the Schmidt value $-0.613\ \mu_N$ for various nuclei due to the small effect from the lower component in the Dirac spinor [26]. Noncharged particles decrease the hypernuclear magnetic moment while charged particles increase it [16]. The prediction for $\mu_{\rm core}$ is smaller than that for $\mu_{\rm core}^\flat$, except ${}^{28}_{\Lambda}$Si and ${}^{32}_{\Lambda}$S show that the proton contributes relatively less to the core polarization in a time-odd triaxial RMF approach than in a perturbation treatment. The sum of contrary contributions from charged and noncharged particles can reverse the sign of the hypernuclear magnetic moment; see results for ${}^{16}_{\Lambda}$O, ${}^{32}_{\Lambda}$S, ${}^{51}_{\Lambda}$V, ${}^{139}_{\Lambda}$La, and ${}^{208}_{\Lambda}$Pb in Table III.

For subshell closed nuclei (${}^{28}_{\Lambda}$Al, ${}^{28}_{\Lambda}$Si, and ${}^{32}_{\Lambda}$S), open-shell nuclei (${}^{51}_{\Lambda}$V, ${}^{89}_{\Lambda}$Y, and ${}^{139}_{\Lambda}$La), deformation, configuration mixing, etc., need to be considered. The last column in Table III is the quadrupole deformation (β, γ) of hypernuclei. According to the perturbation treatment, core polarization introduces a reduction factor in the Dirac magnetic moment μ_D as $B_f(r) = \frac{g_{\omega\Lambda}}{g_{\omega N}}\frac{m_N}{m_\Lambda}[1 + \frac{m_\omega^2 E_F^*}{g_{N\omega}^2 \rho_N}]^{-1}$ with the density distribution of the nuclear core ρ_N and the Fermi energy $E_F^* = \sqrt{[\frac{3\pi^2}{2}\rho_N(r)]^{2/3} + (m^*)^2}$ [14,29]. We found the ground state for ${}^{28}_{\Lambda}$Si located around $\beta = -0.3$ and that for ${}^{32}_{\Lambda}$S located around $\beta = 0.2$ with a constrained axial RMF + BCS approach [30]. The former prediction is consistent with a deformed Skyrme Hartree-Fock (SHF) prediction [31]. For excited ${}^{28}_{\Lambda}$Si ($\beta \simeq 0.2$) and ${}^{32}_{\Lambda}$S ($\beta \simeq -0.1$) predicted here, the large Fermi energy causes a decreased reduction factor in μ_D and core polarization is suppressed; see data in Table III. Lu *et al.* [32] found the addition of a Λ hyperon in light nuclei alters slightly the location of the ground-state minimum towards the direction of smaller β and softer γ in the potential energy surface $E(\beta, \gamma)$. We assume the deformation of nuclei presented in Table III has few changes via the potential energy surface. Thus, the case where the proton contributes more to the magnetic moment than the noncharged neutron and hyperon in deformed ${}^{28}_{\Lambda}$Si and ${}^{32}_{\Lambda}$S can still exist.

The isoscalar magnetic moment can provide us evidence of the second-order configuration mixing (tensor correlation), which is a factor contributing to the difference between the Schmidt values and the experimental data [33]. By averaging the moments of corresponding states in mirror nuclei, the vector contributions are canceled, revealing the isoscalar component, viz., $\mu_{\rm IS}(A) = [\mu(Z, N) + \mu(Z+1, N-1)]/2$. And the isovector magnetic moment is $\mu_{\rm IV}(A) = [\mu(Z, N) - \mu(Z+1, N-1)]/2$. For mirror nuclei ${}^{28}_{\Lambda}$Al and ${}^{28}_{\Lambda}$Si in Table III,

TABLE IV. Magnetic moment in excited hypernuclei with a double-closed core. Results are obtained with the parameter set PK1-Y1 using the time-odd triaxial RMF approach. The Schmidt value $\mu_{\text{Sch.}}$ is $-0.613\,\mu_N$. The deviation of the hypernuclear magnetic moment from the Schmidt value is $\Delta\mu = \mu_{\text{tot.}} - \mu_{\text{Sch.}}$. Λ single-particle energy ε_Λ marked by an asterisk refers to the excited case when Λ occupies the lowest $l_\Lambda = 1$ orbit.

Nuclei	ε_Λ	μ_D	μ_a^Λ	$\mu_{\text{tot.}}$	$\Delta\mu$
${}^{17}_{\Lambda}$O	−2.924*	−0.030	−0.580	−0.610	0.003
${}^{41}_{\Lambda}$Ca	−10.229*	−0.071	−0.608	−0.688	−0.075
${}^{57}_{\Lambda}$Ni	−14.097*	−0.014	−0.576	−0.590	0.023
${}^{133}_{\Lambda}$Sn	−19.514*	−0.016	−0.521	−0.537	0.076
${}^{209}_{\Lambda}$Pb	−21.750*	−0.051	−0.571	−0.622	−0.009
${}^{17}_{\Lambda}$O	−12.700	−0.009	−0.610	−0.619	−0.006
${}^{41}_{\Lambda}$Ca	−18.739	−0.014	−0.610	−0.624	−0.011
${}^{57}_{\Lambda}$Ni	−22.072	−0.018	−0.610	−0.628	−0.015
${}^{133}_{\Lambda}$Sn	−24.556	−0.015	−0.611	−0.626	−0.013
${}^{209}_{\Lambda}$Pb	−25.637	−0.016	−0.612	−0.628	−0.015

we have the following:

Obtained via	$\mu_{\text{tot.}}$	$\mu^{\flat}$	$\mu_{\text{Sch.}}$
μ_{IS}	1.1736	0.9986	0.827
μ_{IV}	2.6293	3.6533	3.353

The isoscalar magnetic moment of the mirror pair (${}^{28}_{\Lambda}$Al and ${}^{28}_{\Lambda}$Si) evaluated by the time-odd triaxial RMF approach ($\mu_{\text{tot.}}$) is larger than that given by the perturbation treatment ($\mu^{\flat}$) and by the extreme single-particle prediction ($\mu_{\text{Sch.}}$). In the present calculation, there is no tensor coupling of the isovector meson ρ. A discrepancy exists in the isovector magnetic moment as there are no vertex corrections for the isovector current. Within one major shell, the RMF model including the configuration mixing removes most of the discrepancies for isovector moments while leaving the isoscalar moments in agreement with experiment [34]. The prediction of subshell nuclei needs more investigation.

Apart from the ground-state case, it is interesting to view the deviation of the magnetic moment from the Schmidt value $\Delta\mu$ in excited nuclei. There may be a large deviation $\Delta\mu$ in the Λ hypernucleus with $l_\Lambda \neq 0$, which comes from the nonvanishing Λ convection current term $\psi^\dagger_\Lambda(\overleftarrow{\nabla} - \overrightarrow{\nabla})\psi_\Lambda$ according to a perturbation treatment for the symmetric nuclear matter [35]. A self-consistent calculation with $\omega\Lambda\Lambda$ tensor coupling may clear the uncertainty of the perturbation treatment. By blocking the lowest $1p_{3/2}$ orbit, magnetic moments for ${}^{17}_{\Lambda}$O, ${}^{41}_{\Lambda}$Ca, ${}^{57}_{\Lambda}$Ni, ${}^{133}_{\Lambda}$Sn, and ${}^{209}_{\Lambda}$Pb are obtained with the parameter set PK1-Y1 in the time-odd triaxial RMF approach (see Table IV). The maximum magnitude of $\Delta\mu$ for excited hypernuclei is 12% of the Schmidt value; see ${}^{41}_{\Lambda}$Ca and ${}^{133}_{\Lambda}$Sn. The hypernuclear magnetic moment is close to the Schmidt value by a 2% difference when the Λ hyperon occupies the lowest $l_\Lambda = 0$ orbit; see the second data block in Table IV. The shift of the Λ hyperon from $l_\Lambda = 0$ to $l_\Lambda = 1$ increases the hypernuclear magnetic moment except for ${}^{41}_{\Lambda}$Ca. If deviation $\Delta\mu$ changes from negative to positive, the magnitude of it may decrease. Nuclei ${}^{17}_{\Lambda}$O and ${}^{209}_{\Lambda}$Pb are exact examples. The magnitude of $\Delta\mu$ for their excited state is smaller than that of the corresponding ground state. Thus, the prediction of a large deviation in the Λ hypernucleus with $l_\Lambda \neq 0$ according to a perturbation treatment [35] suits medium-mass nuclei better than the other parts along the nuclear chart.

IV. SUMMARY

Hypernuclear magnetic moments have been studied in the self-consistent time-odd triaxial RMF approach, including the strangeness, the spacelike component, and tensor coupling. The previous prediction that the core-polarized Dirac magnetic moment is restored to the Schmidt value as the hyperon stays at the $l_\Lambda = 0$ state with $\omega\Lambda\Lambda$ tensor coupling is confirmed. The valence Λ hyperon results in a core-polarized proton current and deviates the magnetic moment from the Schmidt value as $\Delta\mu$. The deviation $\Delta\mu$ is related to effective interaction, in particular to Λ-meson coupling strengths $g_{\sigma\Lambda}$ and $g_{\omega\Lambda}$. Contrary contributions from charged and noncharged particles cause a reversed sign of the prediction and the Schmidt value. This may be a signal for future experiments to study. The deviation $\Delta\mu$ of single Λ hypernuclei with p_Λ orbits occupied is large for the medium-mass region, but not for the others.

ACKNOWLEDGMENTS

This work was partly supported by the National Natural Science Foundation of China under Grant No. 11105111, the Chinese Universities Scientific Fund 2011JS050, and Aizu University Scientific Fund R-1-10.

[1] T. Yamazaki, Phys. Lett. B **160**, 227 (1985).
[2] O. Hashimoto and H. Tamura, Prog. Part. Nucl. Phys. **57**, 564 (2006).
[3] P. Achenbach *et al.*, IEEE Trans. Nucl. Sci. **56**, 316 (2009).
[4] F. Garibaldi, O. Hashimoto, J. J. LeRose, P. Markowitz, S. N. Nakamura, J. Reinhold, and L. Tang, J. Phys.: Conf. Ser. **299**, 012013 (2011).
[5] H. Tamura, M. Ukai, T. O. Yamamoto, and T. Koike, Nucl. Phys. A **881**, 310 (2012).
[6] H. Tamura *et al.*, Phys. Rev. Lett. **84**, 5963 (2000).
[7] M. Ukai *et al.*, Phys. Rev. Lett. **93**, 232501 (2004).
[8] T. Fukuda and T. Saito (HypHI Collaboration), Nucl. Phys. A **790**, 161c (2007).
[9] P. G. Reinhard, Rep. Prog. Phys. **52**, 439 (1989).
[10] P. Ring, Prog. Part. Nucl. Phys. **37**, 193 (1996).
[11] D. Vretenar, A. V. Afanasjev, G. A. Lalazissis, and P. Ring, Phys. Rep. **409**, 101 (2005).
[12] J. Meng, H. Toki, S. G. Zhou, S. Q. Zhang, W. H. Long, and L. S. Geng, Prog. Part. Nucl. Phys. **57**, 470 (2006).
[13] J. Cohen and R. J. Furnstahl, Phys. Rev. C **35**, 2231 (1987).

[14] J. M. Yao, H. F. Lü, G. Hillhouse, and J. Meng, Chin. Phys. Lett. **25**, 1629 (2008).
[15] J. Cohen, Phys. Rev. C **48**, 1346 (1993).
[16] X. S. Wang, H. Y. Sang, H. F. Lü, J. M. Yao, and H. Sagawa, Eur. Phys. J. A **49**, 101 (2013).
[17] A. O. Gattone, M. Chiapparini, and E. D. Izquierdo, Phys. Rev. C **44**, 548 (1991).
[18] J. Mareš and J. Žofka, Phys. Lett. B **249**, 181 (1990).
[19] X. S. Wang, H. Y. Sang, J. H. Wang, and H. F. Lü, Commun. Theor. Phys. **60**, 479 (2013).
[20] W. H. Long, J. Meng, N. Van Giai, and S.-G. Zhou, Phys. Rev. C **69**, 034319 (2004).
[21] J. Cohen and H. J. Weber, Phys. Rev. C **44**, 1181 (1991).
[22] B. D. Serot, Phys. Lett. B **107**, 263 (1981).
[23] R. J. Furnstahl and B. D. Serot, Nucl. Phys. A **468**, 539 (1987).
[24] J. M. Yao, H. Chen, and J. Meng, Phys. Rev. C **74**, 024307 (2006).
[25] R. J. Furnstahl, Phys. Rev. C. **38**, 370 (1988).
[26] H. Lü, Chin. Phys. Lett. **24**, 2547 (2007).
[27] J. Mareš and B. K. Jennings, Phys. Rev. C **49**, 2472 (1994).
[28] D. Vretenar, W. Pöschl, G. A. Lalazissis, and P. Ring, Phys. Rev. C **57**, R1060 (1998).
[29] W. H. Long, N. V. Giai, and J. Meng, Phys. Lett. B **640**, 150 (2006).
[30] H. F. Lü, L. S. Geng, and J. Meng, Eur. Phys. J. A. **31**, 273 (2007).
[31] X. R. Zhou, H. J. Schulze, H. Sagawa, C. X. Wu, and E. G. Zhao, Phys. Rev. C **76**, 034312 (2007).
[32] B. N. Lu, E. G. Zhao, and S. G. Zhou, Phys. Rev. C **84**, 014328 (2011).
[33] E. G. Zhao, Chin. Sci. Bull. **57**, 4394 (2012).
[34] U. Hofmann and P. Ring, Phys. Lett. B **214**, 307 (1988).
[35] J. Cohen and J. V. Noble, Phys. Rev. C **46**, 801 (1992).